8-3-2018

Testing Quantum Electrodynamics in the Lowest Singlet State of Neutral Beryllium-9

E. C. Cook
Smith College

Alisha Daya Vira
Smith College

E. Livernois
Smith College

William Williams
Smith College, wraven@smith.edu

Testing Quantum Electrodynamics in the Lowest Singlet State of Neutral Beryllium-9

E. C. Cook, A. D. Vira, C. Patterson, E. Livernois, and W. D. Williams

Phys. Rev. Lett. **121**, 053001 — Published 3 August 2018

DOI: 10.1103/PhysRevLett.121.053001

Testing quantum electrodynamics in the lowest singlet state of neutral beryllium-9

E.C. Cook, A.D. Vira, C. Patterson, E. Livernois, and W.D. Williams*

Physics Department, Smith College, Northampton, MA 01063, USA

(Dated: June 26, 2018)

Abstract

We report spectroscopic results on the $2s2p\ ^1\mathrm{P}_1$ state in neutral atomic beryllium-9. The absolute frequency for the center of gravity is determined to be 42565.4501(13) cm^{-1}, a factor of 130 more precise than the previous experimental measurement. The result is in agreement with and a factor of 8 more precise than the current best theoretical estimate of 42565.441(11) cm^{-1}, which was calculated including the effects of quantum electrodynamics. Due to the large natural linewidth of the transition, the hyperfine constants were not able to be extracted to high precision.

INTRODUCTION

Quantum electrodynamics (QED), the relativistic quantum field theory that describes the interaction between light and matter, is one of the most tested and successful modern theories. There are a variety of completed and ongoing experiments that test the validity of the theory; see [1] for a recent review. In the context of spectroscopy, testing QED typically involves a theoretical prediction of an atomic property, such as the absolute energy of a state, and an experimental verification of the prediction.

Theoretical calculations of atomic properties, such as transition frequencies, generally become more difficult as the neutron, proton, and electron number increase. During the last 80 years, research on the helium and lithium atoms has served to refine various quantum mechanical methods. For helium, the Hylleraas-type quantum mechanical methods [2] have more than 40 digits accuracy and are more precise than the best experiments [3–8]. The accuracy achieved for lithium is up to 14-15 digits [9–14].

While the theoretical precision for beryllium still lags behind the other light elements, recent improvements in theoretical methods have resulted in predictions for several energy levels that exceed current experimental results [15, 16]. Puchalski et al., using fully correlated Gaussian basis sets while taking into account relativistic, quantum electrodynamics (QED), and finite nuclear mass effects, calculated the neutral beryllium-9 $2s^2\,{}^1\mathrm{S}_0 - 2s2p\,{}^1\mathrm{P}_1$ transition energy to be 42565.441(11) cm^{-1} [15]. The QED shift was 1.048(9) cm^{-1}, a prediction verified from this measurement.

The most precise experimental measurements of most of the energy levels of neutral beryllium-9 occurred over 50 years ago. In 1953, Bozman et al measured the $2s^2\,{}^1\mathrm{S}_0 - 2s2p\,{}^3\mathrm{P}_1$ transition to have energy 21978.925(10) cm^{-1} [17]. In 1962, Johansson performed measurements of many transitions with 0.01–0.02 Å precision; the $2s^2\,{}^1\mathrm{S}_0 - 2s2p\,{}^1\mathrm{P}_1$ transition energy was measured to be 42565.35(18) cm^{-1} [18]. In 1983, Beigang et al. improved upon the work of Seaton by determining the ionization potential of beryllium to be 75192.64(6) cm^{-1} [19, 20].

In this letter, a frequency-doubled Ti:sapphire laser referenced to a calibrated, temperature-stabilized, ultra low expansion (ULE) optical cavity [21] is used to perform Doppler-free spectroscopy on the $2s^2\,{}^1\mathrm{S}_0 - 2s2p\,{}^1\mathrm{P}_1$ transition in neutral beryllium-9. For this work, the absolute laser frequency is known to ±2.8 MHz. Due to the large natural linewidth of

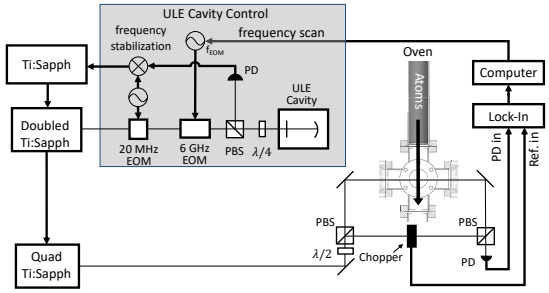

FIG. 1. Simplified experimental setup. The frequency doubled light near 470 nm is referenced and controlled by the calibrated, temperature stabilized ULE cavity. The quadrupled light near 235 nm is used for spectroscopy on an atomic beam of neutral beryllium-9.

this transition, the hyperfine spectral features overlap. We report a conservative center-of-gravity transition energy of 42565.4501(13) cm^{-1}, in agreement with the latest theoretical prediction and verifying the need for inclusion of QED contributions [15]. The merged hyperfine structure prevents extraction of the hyperfine coefficients and limits the precision with which the absolute frequency can be determined.

METHOD AND EXPERIMENTAL SETUP

The experimental design, see Fig. 1, is composed of two main components: a saturated absorption spectroscopy setup for the beryllium atom beam and a dual frequency modulation setup to stabilize and scan the laser frequency with respect to the ULE cavity. The atomic beam is produced in an oven (CreaTec Fisher & Co. DFC-40-10-WK-2B) composed of a tantalum crucible containing a 30-mm long $\times$ 3-mm diameter collimating tube and a further 3-mm diameter collimating aperture 50 mm from the end of the collimating tube. The oven is controlled with two separate heating elements, one for the crucible, held at 1200°C, and the second for the lip of the collimating tube, held at 1225°C. The beam diverges at $\sim$13 mRad, resulting in a transverse temperature of less than 1 K.

A frequency-quadrupled Ti:sapphire laser (MSquared SOLSTIS and doubling cavities ECD-X and ECD-X-Q) is used to produce 234.9 nm light for saturated absorption spectroscopy on beryllium-9. The pump and probe beams are split and combined with polarizing beam splitters to ensure overlap for 1.7 m, resulting in a pump/probe parallel uncertainty

of ≤ 0.5 mrad. Combined with the atomic beam pointing angle uncertainty of ≤ 10 mrad, the residual Doppler shift is ≤ 50 kHz. The 10-mW pump beam is elliptical with a horizontal $1/e^2$ waist of 1.1 mm and a vertical waist of 0.6 mm. The pump beam is chopped with a mechanical chopper (Stanford Research Systems SR540) at $\sim$3.2 kHz. The probe beam has $\sim$500 μW of light with waists similar to the pump beam. The probe light passes through the atomic beam followed by a polarizing beam splitter before hitting a photodetector (Thorlabs PDA36A), which monitors the transmitted probe beam. The output of the photodetector is demodulated at the pump beam chopping frequency by a lock-in amplifier (Stanford Research Systems SR830).

To control and measure the frequency of the laser, frequency-doubled light from the Ti:sapphire laser at 469.9 nm is referenced to a calibrated, temperature-stabilized ultra-low-expansion (ULE) cavity [21]. Dual frequency modulation is used to both stabilize and scan the frequency of the laser light [22]. The light is modulated by a resonant 20 MHz electro-optical modulator (EOM) (Photonics Technologies LTD EOM-01-20-U) followed by a temperature-stabilized high-frequency fiber EOM (6 GHz bandwidth, AdvR Inc WPM-P48P48-AL0-488nm) driven by a computer-controlled function generator (Stanford Research Systems RF signal generator SG384). The reflected light from the ULE cavity is detected and demodulated at 20 MHz by a commercial photodetector/demodulation unit (Stable Laser Systems PDH-1000-20B) using a standard Pound-Drever-Hall (PDH) setup [23].

The $2s^2\ {}^1\mathrm{S}_0 - 2s2p\ {}^1\mathrm{P}_1$ spectral feature falls between two cavity modes, f_n and f_{n+1}; the cavity mode frequency is doubled to determine the frequency of the 234.9-nm light. To control the frequency of the laser, the negative sideband of the high-frequency EOM is stabilized to the lower frequency cavity mode, f_n. The frequency of the light, f_L, interrogating the beryllium atoms is given by

$$f_L = 2 * (f_n + f_{\mathrm{EOM}}), \tag{1}$$

where f_{EOM} is the frequency driving the high-frequency EOM. Thus scanning the frequency of the high-frequency EOM results in scanning the laser itself. The procedure and results for determining the frequency of the ULE cavity modes are described by Patterson et al. [21].

RESULTS

The frequency-doubled Ti:sapphire laser is stabilized to the ULE cavity as described in the method and experimental setup section and scanned across the spectral feature. Each data point is collected by averaging the transmitted probe beam signal for 100 ms before stepping the EOM frequency by 1 MHz (2 MHz at 235 nm). A settling time of 100 ms is used between data points. The laser is alternately scanned both up and down in frequency to check for hysteresis effects from the lock-in amplifier. No hysteresis effects were seen. Figure 2 shows an example of a typical sub-Doppler spectrum. The 1-sigma uncertainty on the absolute frequency of the laser is ±2.8 MHz. The error budget for the absolute frequency of the laser is shown in Table I. There are four contributions to the frequency uncertainty: determination of the cavity mode frequency from the original cavity calibration [21], cavity drift between calibration and the current experiment, the Pound-Drever-Hall (PDH) lock offset uncertainty, and the residual Doppler shift uncertainty which arises from imperfect atomic beam pointing and pump/probe laser beam overlap.

The original ULE cavity calibration allows determination of the cavity mode frequency f_n to an accuracy of 1.37 MHz. The cavity drift is monitored by repeating absolute frequency measurements on a sampling of the $6s_{1/2} - 7p$ lines in neutral cesium-133 measured during the original cavity calibration. The average of the individual line drifts indicates an overall cavity drift of 1.964(63) MHz and is a systematic effect of our measurement. The laser is stabilized to a given cavity mode to better than 30 kHz, with the limit imposed by offset

TABLE I. Systematic and statistical measurement uncertainties (one standard deviation) for the absolute frequency at 469.9 nm; the overall uncertainty is then doubled for the 234.9 nm light.

Frequency Calibration Error Source	(kHz)
ULE cavity mode uncertainty	1370
Cavity mode drift uncertainty	60
PDH offset drift	30
Residual Doppler shift	50
Overall (quadrature sum)	2×1400 kHz
Overall in cm^{-1}	0.00009 cm^{-1}

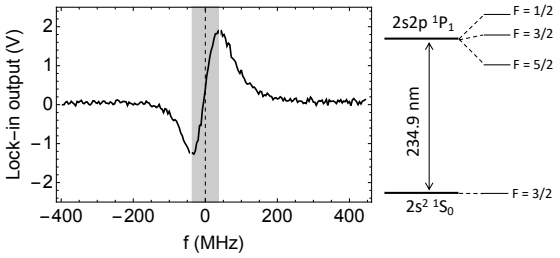

FIG. 2. A typical Doppler-free spectrum. 0 MHz on the horizontal axis is referenced to 1,276,080,091.7(2.8) MHz, or 42565.45012(9) cm^{-1}. The shaded area indicates a conservative range for the center of gravity. The center of the shaded area, indicated by the dotted line, is halfway between the spectra minimum and maximum; see text for more details. A simplified Grotrian diagram (not to scale) is also shown.

drift of the PDH error signal (arising from residual amplitude modulation in the 20 MHz EOM).

Figure 2 shows the Doppler-free spectrum of the $2s^2\,{}^1\mathrm{S}_0 - 2s2p\,{}^1\mathrm{P}_1$ transition for the experimental parameters given above. The shape of the spectrum, which resembles but is not a derivative signal, is partially due to polarization-dependent optical-pumping effects. The traditional Doppler-free spectrum would be assumed to be composed of 6 overlapping spectral features, 3 hyperfine transitions and 3 crossover features, that would typically be fitted to determine the absolute transition frequency and the magnetic dipole and electric quadrupole hyperfine constants. In this case, the natural linewidth is larger than the hyperfine splitting, and the Doppler-free spectrum has merged features. The transition rate was calculated to be 5.52×10^8 s^{-1} ($2\pi\times87$ MHz) with an uncertainty of less that 3% [24, 25], in agreement with the $2\mathrm{s}2\mathrm{p}\,{}^1\mathrm{P}_1$ lifetime measurement of 1.85(4) ns [26]. The hyperfine splitting from the center of gravity is given by

$$W = \frac{1}{2}A\,K + B\,\frac{(3/2)K(K+1) - 2I(I+1)J(J+1)}{2I(2I-1)2J(2J-1)}, \tag{2}$$

where $K = F(F+1) - I(I+1) - J(J+1)$, A is the magnetic dipole constant, B is the electric quadrupole constant, I is the nuclear spin, J is the total electronic angular momentum, and F is the total atomic angular momentum.

Due to the merged spectral features, we are unable to extract the hyperfine constants to high precision, which in turn constrains the precision with which we can determine the absolute frequency. We estimate the center of gravity to be between the minimum and

maximum features seen in Figure 2. We therefore report the absolute frequency of the center of gravity to be halfway between these features with uncertainty given by half of the frequency difference between the minimum and maximum. The absolute transition frequency for the center of gravity of the $2s^2\,{}^1\mathrm{S}_0 - 2s2p\,{}^1\mathrm{P}_1$ transition is found to be 1,276,080,092(40) MHz, or 42565.4501(13) cm^{-1}, an improvement of 130 over the best previous value [18].

DISCUSSION AND CONCLUSION

The absolute frequency for the center of gravity for the $2s^2\,{}^1\mathrm{S}_0 - 2s2p\,{}^1\mathrm{P}_1$ transition agrees with the current best theoretical prediction, a confirmation of both QED and the theoretical methods used to determine the energy of the transition. The current experimental measurement is a factor of 8 more precise than the theoretical prediction and will provide guidance for further improvements on the theoretical methods used for multi-electron atoms.

A level-crossing experiment can provide both the hyperfine coefficients and a higher-precision measurement of the center-of-gravity frequency [27, 28]. Many other beryllium energy levels remain to be explored; the $2s2p\,{}^3\mathrm{P}_J$ states are of particular theoretical interest but have yet to be measured to high precision [24, 29–31]. The lifetime of the 2s2p $^1\mathrm{P}_1$ state has been measured experimentally to 2% precision and calculated to 3% precision [24–26]. However, the lifetime of the 2s2p $^3\mathrm{P}_1$ state has not yet been measured experimentally, and the uncertainty on the calculation of the lifetime of the 2s2p $^3\mathrm{P}_1$ state is quite large [24, 25]. Future precision spectroscopy on beryllium-9 promises to further test our understanding of atomic structure and QED effects.

This work was supported by the National Science Foundation through grant numbers PHY-1428112 and PHY-1555232.

* wwilliams@smith.edu

[1] M. Safronova, D. Budker, D. DeMille, D. F. J. Kimball, A. Derevianko, and C. W. Clark, Rev. Mod. Phys. (2018).

[2] E. A. Hylleraas, Zeitschrift für Physik **54**, 347 (1929).

[3] D. Shiner, R. Dixson, and V. Vedantham, Phys. Rev. Lett. **74**, 3553 (1995).

[4] L.-B. Wang, P. Mueller, K. Bailey, G. W. F. Drake, J. P. Greene, D. Henderson, R. J. Holt,

R. V. F. Janssens, C. L. Jiang, Z.-T. Lu, T. P. O'Connor, R. C. Pardo, K. E. Rehm, J. P. Schiffer, and X. D. Tang, Phys. Rev. Lett. **93**, 142501 (2004).

[5] P. Mueller, I. A. Sulai, A. C. C. Villari, J. A. Alcántara-Núñez, R. Alves-Condé, K. Bailey, G. W. F. Drake, M. Dubois, C. Eléon, G. Gaubert, R. J. Holt, R. V. F. Janssens, N. Lecesne, Z.-T. Lu, T. P. O'Connor, M.-G. Saint-Laurent, J.-C. Thomas, and L.-B. Wang, Phys. Rev. Lett. **99**, 252501 (2007).

[6] G. W. F. Drake, M. M. Cassar, and R. A. Nistor, Phys. Rev. A **65**, 054501 (2002).

[7] C. Schwartz, Int. J. Mod. Phys. E **15**, 877 (2006).

[8] H. Nakashima and H. Nakatsuji, J. Chem. Phys. **128**, 154107 (2008).

[9] J. S. Sims and S. A. Hagstrom, Phys. Rev. A **80**, 052507 (2009).

[10] M. Puchalski, D. Kedziera, and K. Pachucki, Phys. Rev. A **80**, 032521 (2009).

[11] K. L. Sharkey, S. Bubin, and L. Adamowicz, Phys. Rev. A **83**, 012506 (2011).

[12] S. Bubin and L. Adamowicz, J. Chem. Phys. **136**, 134305 (2012).

[13] L. M. Wang, Z.-C. Yan, H. X. Qiao, and G. W. F. Drake, Phys. Rev. A **85**, 052513 (2012).

[14] M. Puchalski, D. Kedziera, and K. Pachucki, Phys. Rev. A **87**, 032503 (2013).

[15] M. Puchalski, J. Komasa, and K. Pachucki, Phys. Rev. A **87**, 030502 (2013).

[16] M. Stanke, J. Komasa, S. Bubin, and L. Adamowicz, Phys. Rev. A **80**, 022514 (2009).

[17] W. R. Bozman, C. H. Corliss, W. F. Meggers, and R. E. Trees, J. Res. Natl. Bur. Stand. **50**, 131 (1953).

[18] L. Johansson, Arkiv Fysik **23**, 119 (1962).

[19] R. Beigang, D. Schmidt, and P. J. West, J. Phys. Colloques **44**, C7 (1983).

[20] M. J. Seaton, J. Phys. B **9**, 3001 (1976).

[21] C. Patterson, A. D. Vira, M. T. Herd, W. B. Hawkins, and W. D. Williams, Rev. Sci. Instrum. **89**, 033107 (2018).

[22] J. I. Thorpe, K. Numata, and J. Livas, Opt. Express **16**, 15980 (2008).

[23] R. W. P. Drever, J. L. Hall, F. V. Kowalski, J. Hough, G. M. Ford, A. J. Munley, and H. Ward, Applied Physics B **31**, 97 (1983).

[24] G. Tachiev and C. F. Fischer, J. Phys. B **32**, 5805 (1999).

[25] J. R. Fuhr and W. L. Wiese, J. Phys. Chem. Ref. Data **39**, 013101 (2010).

[26] R. Schnabel and M. Kock, Phys. Rev. A **61**, 062506 (2000).

[27] F. D. Colegrove, P. A. Franken, R. L. Lewis, and R. H. Sands, Phys. Rev. Lett. **3**, 420 (1959).

[28] H.-J. Kluge and H. Sauter, Zeitschrift für Physik **270**, 295 (1974).

[29] K. T. Chung and X.-W. Zhu, Phys. Rev. A **48**, 1944 (1993).

[30] F. J. Gálvez, E. Buendía, and A. Sarsa, J. Chem. Phys. **118**, 6858 (2003).

[31] A. M. Frolov and M. B. Ruiz, Chem. Phys. Lett. **595-596**, 197 (2014).